DREO

RESEARCH AND DEVELOPMENT BRANCH

DEPARTMENT OF NATIONAL DEFENCE
CANADA

DEFENCE RESEARCH ESTABLISHMENT OTTAWA

TECHNICAL NOTE 80-31

14 / DREO--TT-?p-??

TECHNIQUE FOR CALIBRATING MINIATURE ELECTRIC-FIELD PROBES FOR USE IN MICROWAVE BIOEFFECTS STUDIES AT 2450 MHz: EVALUATION AND CALIBRATION OF BRH — NARDA PROBES.

by

Douglas A./Hill   George W. Hartsgrove

Radiation Biology Section
Protective Sciences Division, DREO

and

G.W. Hartsgrove

Division of Biological Sciences,
National Research Council, Ottawa

PROJECT NO.
16C

OCT⬛⬛⬛⬛980
OTTAWA

FOREWORD

This work was performed in the laboratories of the Division of Biological Sciences, National Research Council of Canada, Ottawa, Canada as part of co-operative DND-NRC studies of the biological effects of nonionizing radiation.

The report is written so that those who are only interested in using calibrated probes of the BRH - Narda type need only read Chapter 1, Section 2.3 and Chapters 5 and 6.

The remainder of the report will be of interest primarily to those who are involved in the design, construction, evaluation and calibration of implantable miniature electric-field probes.

iii

ABSTRACT

A set of miniature probes for determining electric fields in tissue was evaluated and calibrated for use in microwave bioeffects studies at 2450 MHz. The calibrations in air and tissue-equivalent liquids were carried out using a new S-band waveguide technique. The air calibration using waveguide has an accuracy of $\pm$10% compared to $\pm$18% for our anechoic-chamber calibration. The average probe sensitivity in air is 1.0 mV/mWcm^{-2} for the five probes calibrated and varies slightly with power density and probe. To estimate probe sensitivity in tissue, a section of waveguide is filled with a tissue-equivalent liquid and is separated from the air-filled waveguide by a very thin (0.25 mm) planar spacer. The probe response is measured as a function of position on either side of the spacer and extrapolated to the interface. The ratio of probe sensitivity in air to that in test liquid is then determined using the continuity of tangential E field across the spacer. Liquids with dielectric properties simulating both wet and dry tissues were used. For the water-glycerol solution modelling wet tissue the probes are 3.0 $\pm$ 0.6 times more sensitive to E^2 than for air. When used in tissue the total calibration error is estimated to be $\pm$30% for E^2 and $\pm$40% for the specific absorption rate at the site. One of the problems with this probe design, the mechanical weakness near the tip, has been eliminated in newer designs. The other problem, that the size of the probe tip ($\sim$3 mm) is too large for optimal use in small-animal organs, is more difficult to solve.

[Handwritten annotations: "+ or –", "1.0 mV/mW per sq. cm", "+ or –", "E superscript + 2", "(approximately)"]

RÉSUMÉ

On a évalué et étalonné un ensemble de sondes miniatures, utilisées pour déterminer les champs électriques dans des tissus, afin d'étudier les effets biologiques des micro-ondes à 2450 MHz. Les étalonnages dans l'air et dans des liquides équivalant à des tissus ont été effectués au moyen d'une nouvelle technique de guide d'ondes de la bande S. La précision de la calibration dans l'air est de ± 10% comparativement à ± 18% pour l'étalonnage dans notre chambre anéchoïque. La sensibilité moyenne de la sonde dans l'air est 1,0 mV/mW cm^{-2} pour les cinq sondes étudiées, et elle varie légèrement en fonction de la densité de puissance et la sonde utilisée. Pour estimer la sensibilité de la sonde dans un tissu, on remplit une section de guide d'ondes avec un liquide équivalent à un tissu et on l'isole du guide d'ondes rempli d'air avec un espaceur plan très mince (0,25 mm). La réponse de la sonde est mesurée en fonction de sa position de chaque côté de l'espaceur et extrapolée à l'interface. Le rapport de la sensibilité de la sonde dans l'air à celle dans le liquide d'essai est ensuite établi en faisant appel à la continuité du champ E tangentiel à travers l'espaceur. On a employé des liquides ayant des propriétés diélectriques simulant des tissus secs et humides. Dans la solution eau-glycérol représentant un tissu humide, on a trouvé que les sondes étaient 3,0 ± 0,6 fois plus sensibles à E^2 que dans l'air. Employées dans des tissus, on a estimé que l'erreur d'étalonnage totale des sondes est ± 30% pour E^2 et ± 40% pour le taux d'absorption spécifique à l'emplacement de mesure. Un des deux problèmes propres à cette sonde, soit la faible résistance mécanique près de l'extrémité, a été résolu au moyen de nouvelles formes. L'autre problème, c'est-à-dire extrémité trop grosse (∼3 mm) pour être utilisée convenablement dans les petits organes d'animaux, est plus difficile à résoudre.

TABLE OF CONTENTS

TABLE OF CONTENTS – Continued

ACKNOWLEDGEMENTS

1. INTRODUCTION

1.1 GENERAL

For microwave bioeffects research it is desirable to know the <u>local</u> rate of energy deposition at the site of action of the microwave radiation. The rate of energy deposition is usually expressed as a specific absorption rate, SAR (W/kg), and is known from the basic physics to be given by

$$SAR = (\sigma/\rho) \ E_T^2 \tag{1}$$

where E_T is the total electric field-strength (rms V/m), σ is the electrical conductivity (mho/m) and ρ is the density (kg/m^3) of the medium. Since σ and ρ are both known quantities, a measure of E_T^2 in the medium gives the SAR.

Amongst others, Bassen and co-workers (1,2) have produced several versions of implantable miniature electric field sensors and have evaluated them for the cases of plane-wave irradiation in air and in tissue-equivalent models.

1.2 GOALS OF THIS STUDY

We have obtained seven units of their single-axis dipole design, produced by Narda Microwave Corporation. The aims of this study are: (i) to develop and evaluate an S-band-waveguide calibration technique for a 2450-MHz calibration of the probes for use both in air and in tissue; (ii) to evaluate the performance and utility of this particular probe design, and (iii) to obtain calibration data for our probes.

1.3 PROBE CONSTRUCTION

The probes under evaluation were produced in 1978 by Narda Microwave Corporation as model #25256. The design was that of the (US) Bureau of Radiological Health, so they are also designated as BRH model 10. Our evaluation was of five original probes, numbers 5,6,7,8 and 9, and of two replacement probes, numbers 7B and 8B.

The probe design is shown in Fig. 1, and Fig. 2 gives details of the dipole antenna construction in the tip. The short dipole is constructed of two lengths of gold foil with a total length of 1.5 mm and has a low-barrier Schottky diode as the detecting element. The miniature antenna is encased in a 1.2-mm thick, 2.3-mm wide planar dielectric substrate of dielectric constant $\doteq$ 2 (2). The rectified dc voltage is taken to a dc voltmeter through the two lines shown. They are constructed of high-resistance material to prevent direct sensing of microwave energy by the lines. The dipole is oriented at a 54° angle with respect to the probe's long axis so that three successive rotations of the probe about its own axis by 120° results in dipole orientations in three mutually perpendicular directions.

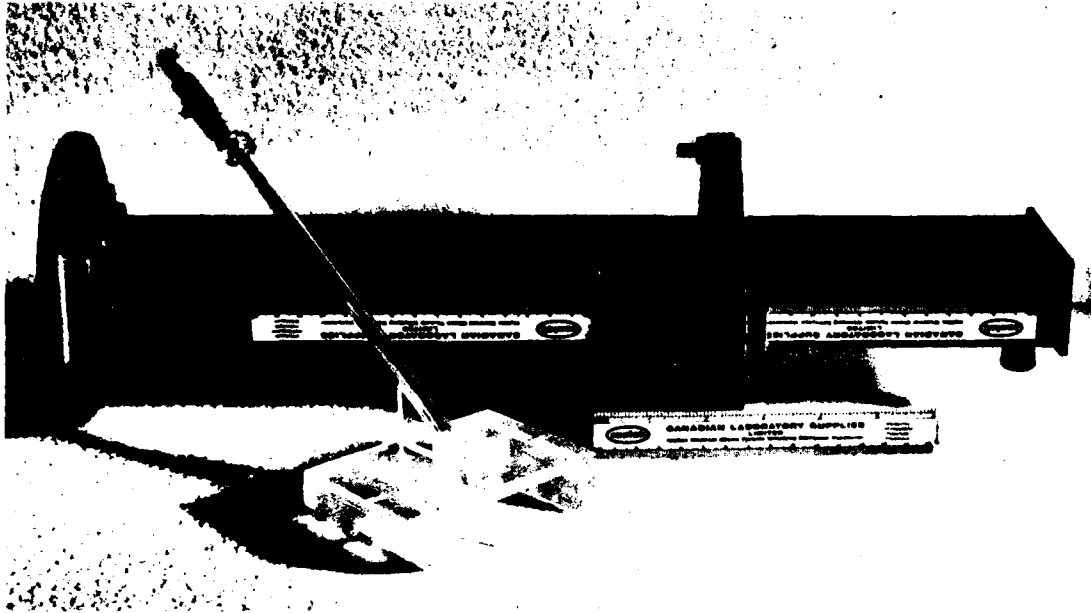Fig. 1. Photo of a miniature electric-field probe in the probe holder used for both waveguide and anechoic-chamber calibration measurements. The slotted waveguide assembly is filled with air to the left of the center flange and with test liquid to the right.
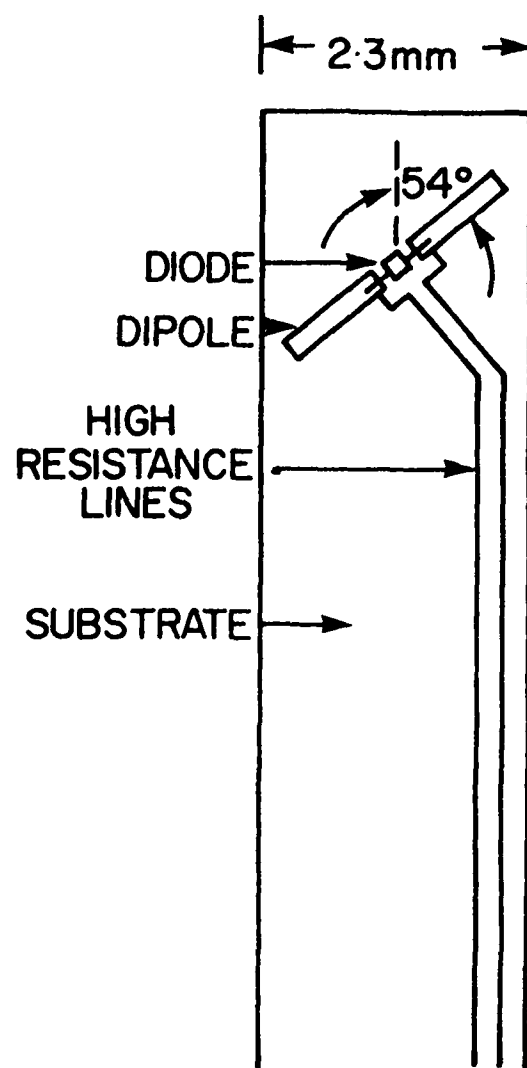
Fig. 2. Design details for the miniature dipole antenna structure in the probe tip (from Bassen, Franke, Aphey and Aslan (2), with permission).

The probe output voltage, V_i, for probe orientation number i ($i = 1,2,3$), is proportional to a power of the electric field-strength, E_i, along the dipole axis for that orientation:

$$V_i = B_M E_i^{2n} \tag{2}$$

where B_M is an empirical constant depending on the medium and $n = 1$ for an ideal diode, 0.95 ± 0.02 in practice. In describing our results we will take n to be 1 and allow B_M to vary slightly with E_i (or V_i).

Summing the three components of Eq. (2) gives the relationship between the total voltage, V_T, and the total electric field, E_T :

$$V_T = B_M E_T^2 \tag{3}$$

1.4 PROBE ELECTRICAL AND MECHANICAL PROBLEMS

At first, probe voltage readings were taken with a high-input-impedance (10^{10} ohms) Keithley Instruments model 610C solid-state electrometer. An RG 174/U miniature coaxial cable was used because of its light weight and flexibility. Cable flexure noise was ± 0.2 mV, causing no problems.

It became clear over a period of six months that the use of the electrometer was occasionally causing the miniature probes to open circuit, or "burn-out" during the process of switching the electrometer off one day and on again the next. An investigation of electrometer performance failed to find any evidence of significant switching transients or abnormal ac or dc currents from the electrometer which might cause this problem.

H. Bassen* advised us that one of his BRH model 10 probes had burned out when the digital voltmeter it was connected to was plugged into the ac power lines. On his advice, we changed to using a Fluke Model 8000A digital multimeter in the battery-operated mode. Probes were never exposed to microwave radiation when not connected to the meter, as a precaution against possible charge accumulation and subsequent discharge. Under these conditions, no more probes have open-circuited. Bassen* believes the 10-20-M-ohm input impedance of the voltmeter is what eliminates the burn-out problem.

In addition to the probe burn-out problem, which destroyed three of our five original probes, a mechanical weakness was found. The joint where the flat 2.5-cm-long end section joins the 3-mm-diameter tube section was weak, resulting in the loss of one probe in the first week of use. The joint was strengthened with epoxy glue in the remaining probes, which were used with as much care as possible, but despite this, one more probe broke at the same place. Bassen et al. (2) reported that several probe tip breakages occurred while probes were pushed through a sphere of tissue-equivalent material. A newer version of the probe, incorporating an epoxy-fiberglass planar tip, has eliminated the breakage problem.*

* private communication

Because of these electrical and mechanical problems with probes as evaluation tests and calibration measurements were proceeding, the test results are incomplete in places. In particular, no useful data was obtained from probes 7 and 8 so only probes 5,6,7B,8B and 9 appear in the tabulated data. At the time of writing, only (replacement) probes 7B and 8B are still operating.

2. CALIBRATION IN AIR-WAVEGUIDE TECHNIQUE

2.1 TECHNIQUE

For the calibration of probe response in air, the measurement system of Fig. 3 was used with the matched load as the final waveguide component. The VSWR of either test cell or matched load was measured with a commercial slotted line. For the matched load, the VSWR is less than 1.04. The probe under test is shown in its holder in Figs. 1 and 3. The 54° angle built into the holder allows one to rotate the probe to the position of maximum response where the dipole is essentially parallel $(\pm 3°)$ to the electric field in the waveguide. Defining the voltage for this orientation as V_1, it was found that the voltages V_2 and V_3 for the other two orientations 120° from the first were small, but not zero. The average result for all probes tested was

$$V_T = V_1 + V_2 + V_3 = (1.07 \pm 0.02) \ V_1. \tag{4}$$

The calibration of V_T vs E_T^2 was then made by first measuring V_T/V_1 for each probe at one power level, and then determining V_1 as a function of E_T^2.

The microwave frequency was determined within ± 3 MHz with a calibrated coaxial transmission wavemeter. The frequency varied during operation, and from day to day, but was always within 15 MHz of 2450 MHz.

Since the dipole antenna is positioned asymmetrically inside a dielectric slab it is possible that wave distortion effects might result in a difference between the readings for a wave approaching the probe "from behind", as in Fig. 3, as compared to a wave approaching from the opposite direction. The measured difference in response was less than 2% and was neglected.

2.2 WAVEGUIDE POWER DENSITY AND ELECTRIC FIELDS

The relationship between the total electric field at the center of the waveguide, E_T, and the net forward power in the waveguide, is derived in Appendix I. The derivation takes into account the fact that the wave impedance for the TE_{10} mode is larger than 377 ohms by the ratio of the guide wavelength to the free-space wavelength. By this measurement the value of B_M for the air medium, designated B_A, was determined. Since the probe is also used to measure the power density in free space, P_d, and since $P_d = E_T^2/377$ (in MKS units) the equation relating V_T to P_d may also
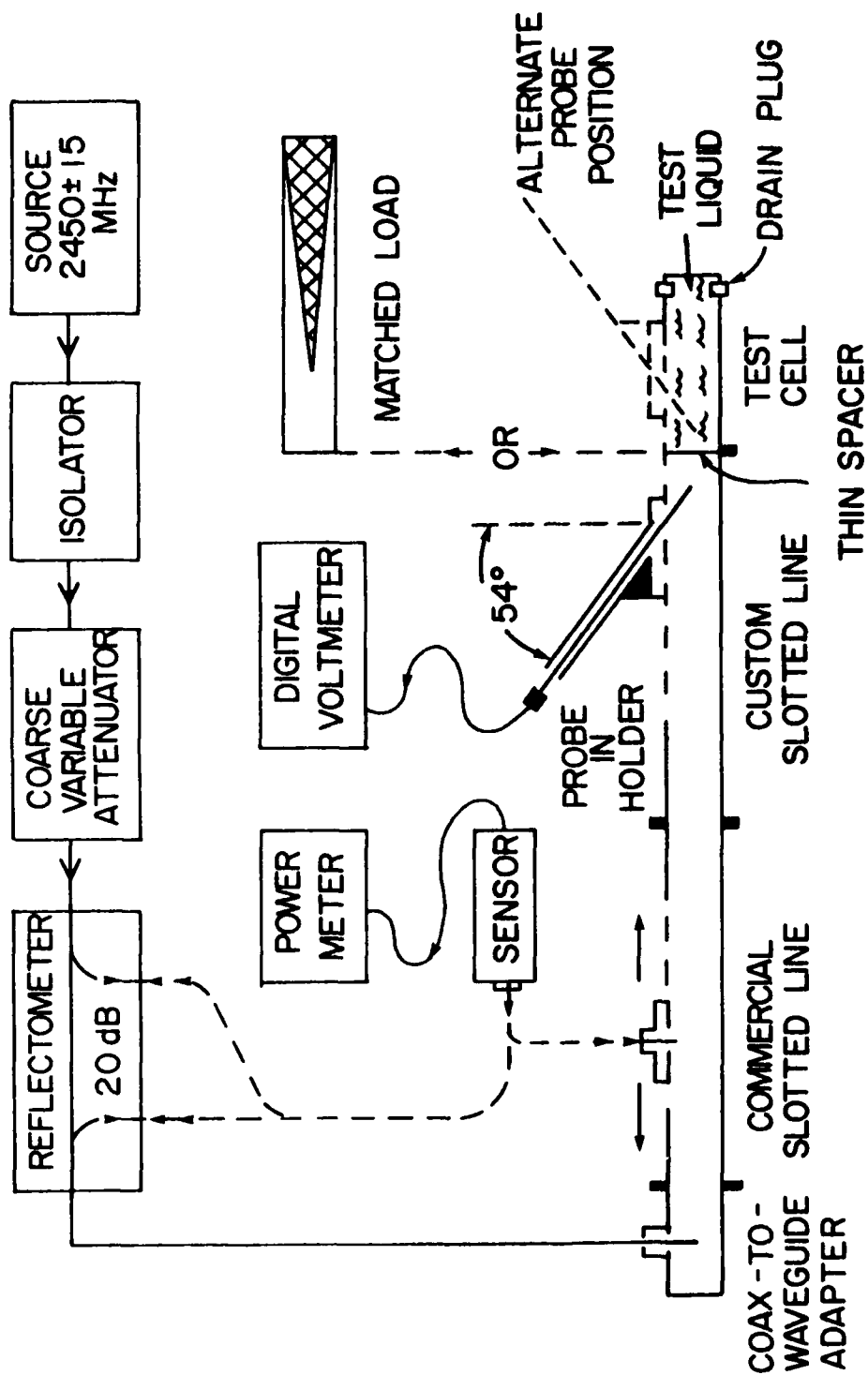
Fig. 3. Hybrid coaxial-waveguide system for probe calibration measurements in air or in test liquids.

be written as:

$$V_T = C_A P_d. \tag{5}$$

C_A depends slightly on the value of P_d (or V_T). Using working units of $mWcm^{-2}$ for P_d, mV for V_T, $mV/mWcm^{-2}$ for C_A and mV/V^2m^2 for B_A, it can be shown that

$$C_A = 3770\ B_A \tag{6}$$

2.3 RESULTS

The resulting calibration curves of V_T vs P_d for probes 7B and 8B are shown as Figs. 4 and 5, respectively. On the log-log plot shown, the points lie on a straight line from about 0.5 to 15 mW/cm^2 with a slope equal to the power-law index, n. The probe response coefficient, $C_A \doteq 1\ mV/mWcm^{-2}$, can be read off the curve at different values of P_d. It has been tabulated along with n for all probes tested at 1, 10 and 50 mW/cm^2 in Table IV of section 3.3, where it is compared to other determinations in air.

The possible errors contributing to the calibration are listed and estimated in Table I, where the best estimate of the total error is shown to be ± 10%.

3. CALIBRATION IN AIR - OTHER TECHNIQUES

3.1 ANECHOIC CHAMBER CALIBRATION

Probes 7B and 8B were also calibrated in the NRC anechoic chamber described by Assenheim and Hartsgrove (3). It was found impractical to calibrate the probes without using a holder for setting position and orientation. The waveguide holder was used, and to average out the inevitable field perturbation effects of the holder, three different configurations of the holder with respect to the incident plane wave, defined in Table II, were used.

The probe, in its holder, was placed on an RF-transparent block of polystyrene foam at a distance of 5.0 m from a large rectangular horn antenna, of nominal gain 22dB. The free-space wavelength for 2450 MHz is $\lambda = 12.2$ cm and the maximum dimension across the face of the horn is d = 64 cm. Using these figures, the distance between the probe and the horn was calculated to be $1.49\ d^2/\lambda$, which puts the probe essentially in the far-field of the antenna.

The anechoic-chamber-calibration results are presented in Table III. Power-density readings performed using either of two Narda Microwave model 8305 radiation monitors or a Holaday Industries model HI 1500 microwave survey meter agreed within 5%. The absolute accuracy of ± 0.5 dB, or ± 12%, stated by Narda Microwave in their manual is assumed to be the main error in power density. The measured probe responses in Table III

8
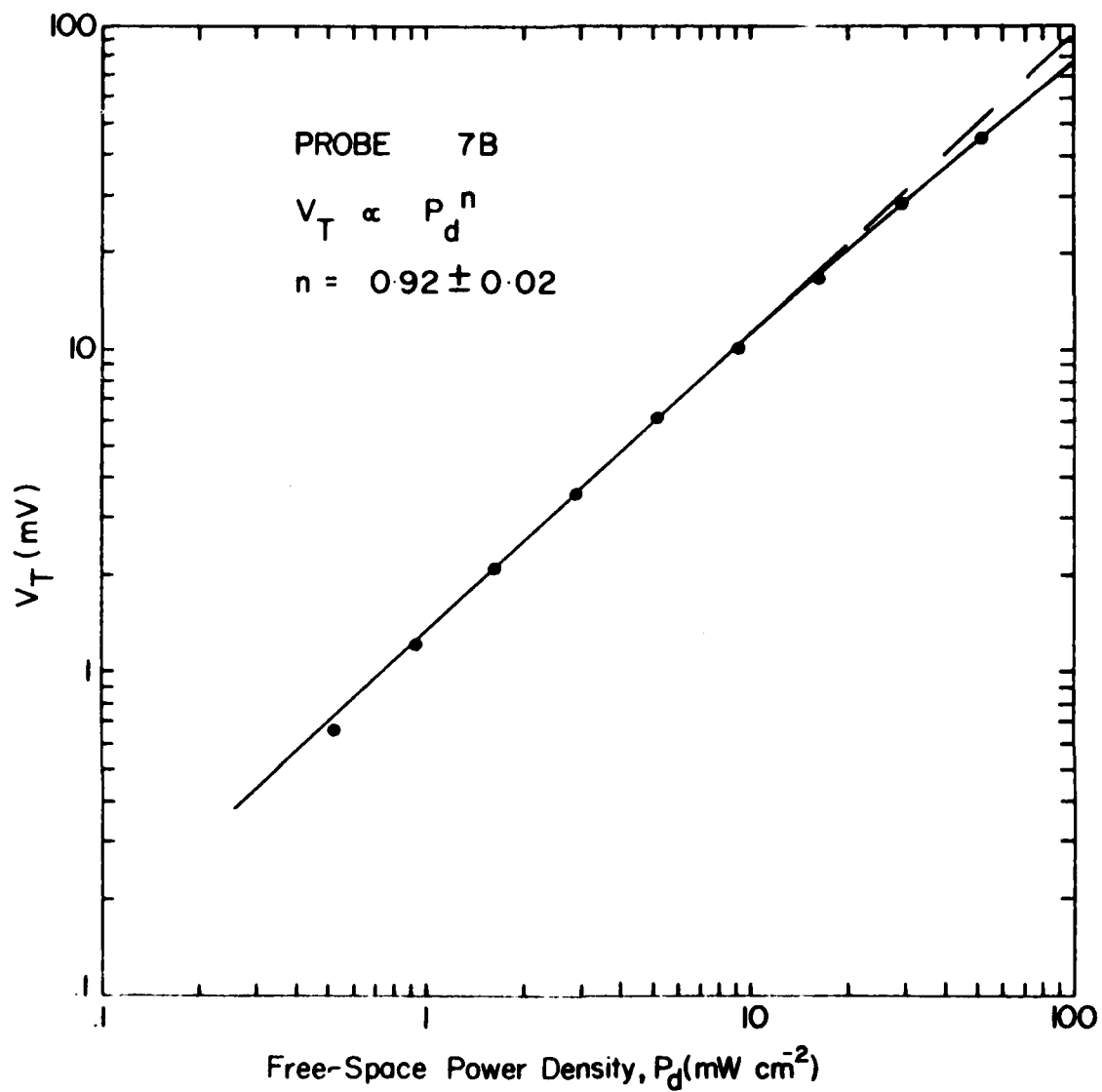
Fig. 4. Calibration curve for the use of probe 7B in air.
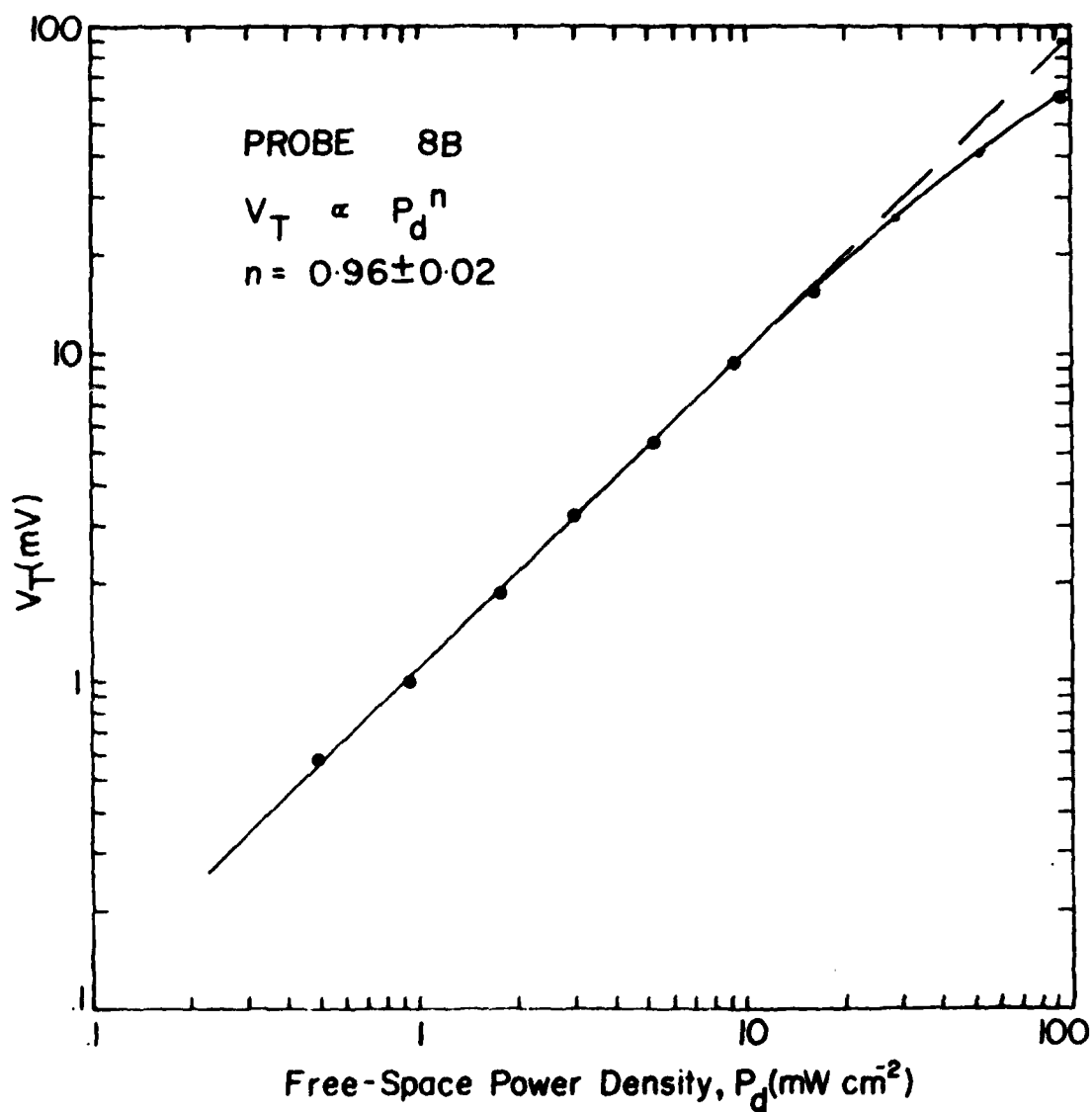
Fig. 5. Calibration curve for the use of probe 8B in air.

TABLE I

Estimated Errors in Waveguide
Calibration Procedure at 2450 MHz

Source of error	Estimated error
Absolute power readings from HP 435A meter,	± 2%
Uncertainty in coupling coefficient of coaxial reflectometer (± 0.2 dB)	± 5%
Variation of correction factor, λ_g/λ, with frequency, 0.2%/MHz over ± 15 MHz,	± 3%
Reproducibility of the ratio, V_T/V_1,	± 3%
From position in the small standing wave pattern (VSMR < 1.05),	± 2%
Estimated Total Error	
Maximum possible (worst-case sum)	±15%
Root-mean-square value,	± 7%
Best estimate (average of the preceeding two estimates)	±11%

TABLE II

Definition of Configuration used for Probe and Holder in
Anechoic Chamber Calibration Measurements

Configuration	Probe axis	Probe holder faces	Probe angle for measurement of V_1
(a)	in EK plane[†]	horn	dipole parallel to E-field
(b)	in EK plane	horn	probe rotated 60° about its own axis from (a)
(c)	in EH plane	sidewall	as for (a)

[†]The electric field, E, is vertical. The magnetic field, H, and direction of propagation of the wave, K, are horizontal.

TABLE III

Anechoic Chamber Calibration Data for Two Probes
Measured at 10 and 50 mW/cm². Frequency is 2450 MHz.

Probe serial number	Power density, P_d (mW/cm²)	Probe configuration defined in Table II	Probe voltage (mV)				C_A (mV/mWcm^{-2})
			V_1	V_2	V_3	V_T	
7B	50 ± 6	(a)	36.6	2.6	0.9	40.1 ± 0.4	
		(b)	0.9	17.6	23.1	41.6 ± 0.3	
		(c)	40.6	4.9	2.6	48.1 ± 0.3	
						43.3 ± 2.5*	0.87 ± 0.16†
	10 ± 1	(a)	10.7	0.6	0.4	11.7 ± 0.2*	1.27 ± 0.23†**
8B	50 ± 6	(a)	30.8	1.8	1.5	34.1 ± 0.3	
		(b)	1.8	17.5	19.8	39.1 ± 0.3	
		(c)	39.2	2.7	2.1	44.0 ± 0.2	
						39.1 ± 2.9*	0.78 ± 0.14†
	10 ± 1	(a)	7.4	0.3	0.2	7.9 ± 0.2*	0.91 ± 0.16†**

* mean ± S.E.

† mean ± 18% : ± 12% from P_d and ± 6% from the S.E.

** mean value calculated by scaling up the single reading in configuration (a) in proportion to the averages determined at 50 mW/cm² for the three configurations.

are indicative of the vertical electric field. The total response, V_T, is seen to depend on configuration. The best estimate of V_T is taken as the mean ($\pm$ S.E.) of the three configurations. The standard error of 6 or 7% in V_T is added to the 12% power density error to give an estimated total error of $\pm$ 18% for C_A.

3.2 NARDA MICROWAVE WAVEGUIDE CALIBRATION

Most of the probes were supplied from Narda Microwave with a C_A value determined at power densities of 1 and 10 mW/cm^2. Their method involved inserting the probe through a small hole in the narrow side of S-band waveguide and positioning it so that the dipole sensed the full electric field at the center of the waveguide. Their C_A values were given for an ideal measuring instrument with infinite input impedance and have been reduced 12% for direct comparison to our data, taken with a 10-Mohm-input-impedance voltmeter.

3.3 COMPARISON OF CALIBRATION DATA IN AIR

The data from the Narda Microwave waveguide calibration, our own waveguide determination and our anechoic-chamber measurements are summarized in Table IV. The C_A values are to be compared keeping in mind the estimated uncertainties of $\pm$ 10% for our waveguide data and $\pm$ 18% for our anechoic-chamber readings. Narda Microwave did not estimate their measurement uncertainty. The data are generally in excellent agreement. Our values for the power-law index lie between 0.01 and 0.04 below those of Narda, but since the uncertainty in each number is $\pm$ 0.02, none of the differences is significant.

4. WAVEGUIDE CALIBRATION IN TISSUE-EQUIVALENT LIQUIDS

4.1 INTRODUCTION

The probes are expected to produce a larger voltage for the same E^2 value in any medium, "M", of dielectric constant, $\epsilon' \gg 1$, than for air. In other words, $B_M = B_M(\epsilon') > B_A$. To evaluate $B_M(\epsilon')$, the end section of waveguide was filled with different test liquids representing a range of ϵ'. The liquid-filled waveguide is separated from the air-filled waveguide by a thin planar spacer inserted between the waveguide flanges. In the air-filled waveguide only the TE_{10} mode exists so that the electric field only has one component, which is tangential to the surface of the spacer, denoted E_t (air). For our probe orientation, V_1 is a measure of E_t (air), i.e.,

$$V_1 \text{ (air)} = B_A E_t^2 \text{ (air)}. \tag{7}$$

Using the boundary condition that the tangential component of E is continuous across any interface, and ignoring (for the moment) any change in E within the thin spacer, the tangential component of E in liquid, E_t (liquid), would be the same value as for air. This should be true regardless of the form of the modes propagating in the liquid-filled waveguide. That is,

$$E_t \text{ (liquid)} = E_t \text{ (air)}. \tag{8}$$

TABLE IV

Summary of Probe Calibration Data for Air

Probe Serial Number	(a) Narda Microwave Data		Our Data: (b) Waveguide					(c) Anechoic Chamber*	
	Power Law Index (n)†	C_A $\left(\dfrac{mV}{mWcm^{-2}}\right)^2$ at 10 mW/cm²	$\dfrac{V_T}{V_1}$	Power Law Index (n)	C_A (mV/mWcm⁻²) at a power density of:			at a power density of: (mWcm⁻²)	
					1	10	50	10	50
5	0.98	1.06	1.07	0.95	1.20	1.07			
6	0.99	1.04	1.07	0.94	1.17	1.01			
7B	-	-	1.10	0.92	1.31	1.10	0.88	1.27 ± 0.23	0.87 ± 0.16
8B	0.98	1.29	1.03	0.96	1.10	1.00	0.80	0.91 ± 0.16	0.78 ± 0.14
9	0.97	0.96	1.06	0.96	0.89	0.82			
mean	0.98	1.09	1.07	0.95	1.13	1.00	0.84	1.09	0.83
(±) S.E.	0.01	0.07	0.01	0.01	0.07	0.05	0.02	-	-

† Derived from the Narda Microwave "% deviation from square law" data.

* Data taken from the last column of Table III.

The response in the liquid medium is given by

$$V_1 \text{ (liquid)} = B_M (\epsilon') E_t^2 \text{ (liquid)} \tag{9}$$

Using Eq. (8) to eliminate the E-fields in equations (7) and (9) we get

$$\frac{B_M (\epsilon')}{B_A} = \frac{V_1 \text{ (liquid, at interface)}}{V_1 \text{ (air, at interface)}} \tag{10}$$

By measuring V_1 as a function of position on each side of the spacer and extrapolating the curves up to the interface, the ratio of probe response coefficients can be determined.

The electric field inside the test liquid is known (see Appendix II) to decay exponentially due to the energy lost in heating the liquid. The characteristic decay length for the electric field, $\delta_1 = \delta_1 (\epsilon', \sigma)$ is defined by the equation

$$E(x) = E(o) \exp(-x/\delta_1) \tag{11}$$

where $E(o)$ is the electric field at the interface and x is the distance into the liquid from the interface.

Since we are measuring $V_1(x)$ which is proportional to the square of $E(x)$ we have

$$V_1(x) = V_1(o) [\exp(-x/\delta_1)]^2$$
$$= V_1(o) \exp(-x/\delta_2) \tag{12}$$

where $\delta_2 = \delta_1/2$ is the exponential decay length for $V_1(x)$. δ_2 has also been measured for the different liquids for comparison to the value calculated (in Appendix II) from the known electrical properties of the liquids.

4.2 TECHNIQUE

An attempt was made to use a thin-walled tray inside the waveguide to contain the test liquid. The results were found to depend critically on the height of the air gap between the top of the liquid and the underside of the waveguide. As a result of this, all tests were done in a specially constructed cell completely filled with test liquid. The slot in the top of the cell is approximately half filled, resulting in a power density radiating out of the slot which is about 1% of the power density in the waveguide. This is neglected in the analysis.

The effect of spacer thickness on the measured quantities B_M/B_A and δ_2 was also tested. There was no detectable difference between the results using a spacer 0.25 mm thick and those using a 1.37-mm-thick spacer. A spacer thickness of 3.0 mm altered the results. The thinnest spacer (0.25 mm) was used in all further tests.

An analysis of preliminary measurements revealed two main sources of error in this procedure - one due to the uncertainty in probe position and the other due to the curve extrapolation process.

To eliminate the uncertainty due to probe position, measurements were taken on each side of the spacer with both sides air-filled. Then the position of each curve from the effective center of the spacer was adjusted for the best-fit curve through the data on both sides of the interface. This procedure reduces the position uncertainty to ± 0.2 mm on each side of the interface.

The other appreciable error results from extrapolating the curves on the air side. The combined uncertainty in the determination of B_M/B_A resulting from these two errors is estimated to range from 0.2 to 0.6. Approximately 2/3 of the error comes from curve extrapolation which in turn depends on curve shape and slope. The worst case, ± 0.6, applies to the water-glycerol solution which represents wet tissue. A computer curve-fitting program would help here, but is not considered to be worth the effort.

4.3 RESULTS

Typical results for $V_1(x)$ measured on both sides of the interface are shown for probe 8B in Fig. 6. As described above, the curves (a) for air have been used to define the best "zero" for distance measurements from the center of the spacer. The curves (b), (c) and (d) using the same zero point show the increased probe response in test liquids. They also show clearly the exponential decay of the voltage in the test liquids, which appears as a good straight line on the semilogarithmic plot. The curved lines on the air side of the interface show the standing-wave pattern in air, which is known to be non-exponential.

The ratio B_M/B_A is taken from the curves extrapolated to the line representing the center of the thin spacer. The results of all such measurements performed on four probes using four test liquids are presented in Table V. Wet tissue can be seen to have electrical properties closest to the glycerol-water solution, which is taken to be the best model of wet tissue in this study. The measurements on glycerol and water were taken to help understand the data for the solution. All tests were done at room temperature, 19-22°C.

All measurements of δ_2 are presented in Table VI. The data show more inconsistency than expected from the estimated uncertainty of about ± 1 mm, even though all curves in liquid were good exponentials. Possible sources of variation include contamination of liquids or the use of liquids not at room temperature.

4.4 DISCUSSION

Regardless of the δ_2 values, the B_M/B_A ratios appear reliable within the error of ± 0.2 to 0.6 stated above. The average response ratio has been tabulated for each test liquid and each probe. There are probably
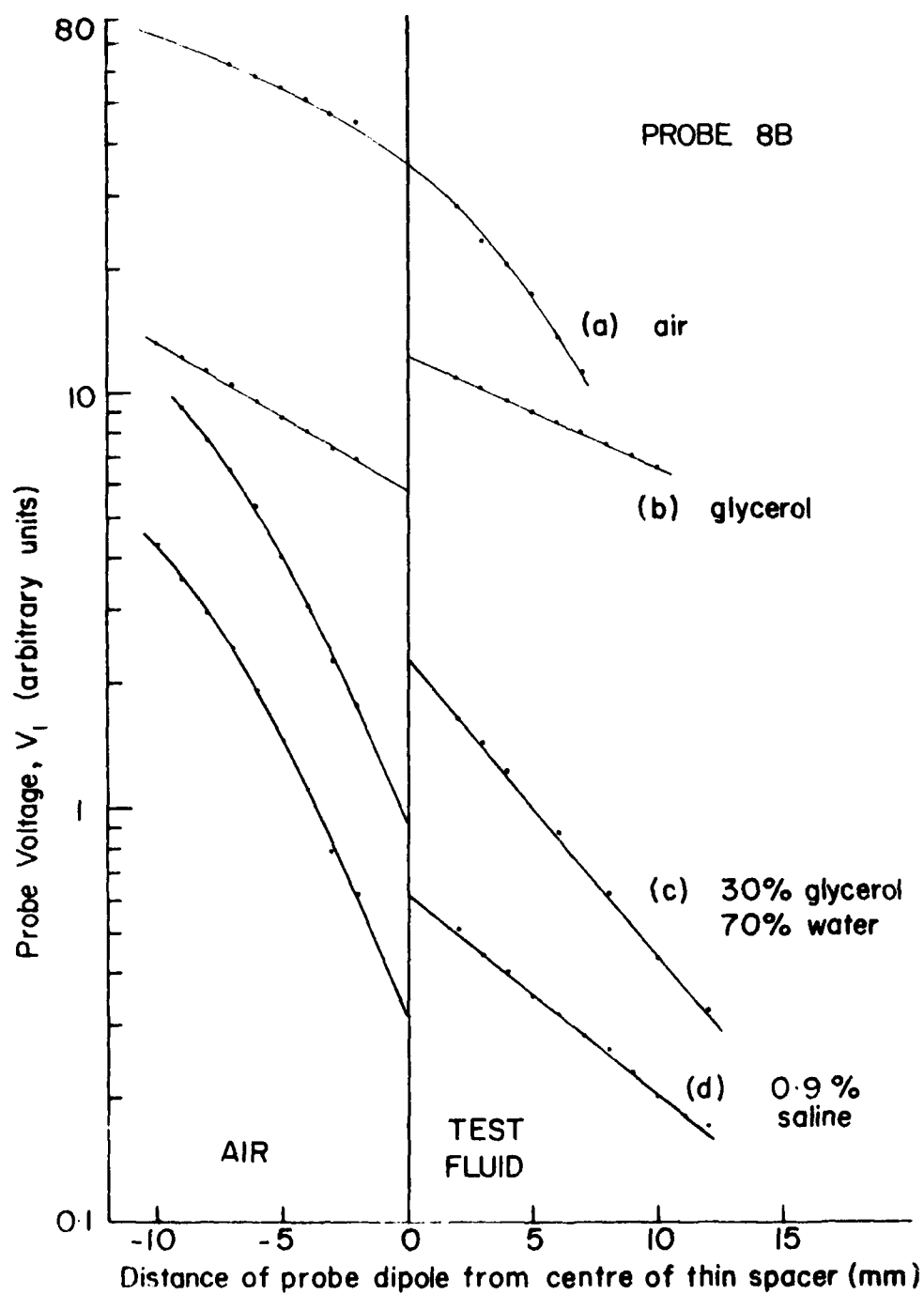
Fig. 6. Probe voltage vs position on both sides of a thin (0.25 mm) spacer separating air from four different test fluids.

TABLE V

Increase in 2,50-MHz Probe Sensitivity, B_M/B_A, in Tissue-Equivalent Liquids. Results for Four Probes Measured in Four Test Liquids

Liquid or material	Dielectric Properties†		B_M/B_A for Probe Number				Average B_M/B_A for liquid (mean ± S.E.)
	ε'	ε''	5	6	7B	8B	
Glycerol	6.3 ± 0.3	3.6 ± 0.4	2.9	3.0	2.6	2.2	2.68 ± 0.18
water:glycerol (70:30 v/v) solution	58.5 ± 1.0	19.5 ± 1.5	3.0	3.9, 2.9	2.8, 3.3	2.5, 2.6	3.00 ± 0.18
testis tissue	45.6 ± 1	13.9 ± 1.5					
0.9% (w/w) saline	74.3	20.5	2.5	2.5	2.3	2.0, 1.8	2.22 ± 0.14
water (20°C)	78.4	10.8	3.0	2.3, 2.2, 2.6	1.9	1.8	2.30 ± 0.18
Probe Average (mean ± S.E.)			2.85 ±0.12	2.77 ±0.22	2.58 ±0.24	2.15 ±0.14	
							Grand Average (N = 22) 2.57 ± 0.11

† From Appendix II

TABLE VI

2450-MHz Depth of Penetration for E_T^2, δ_2

Results for Four Probes Measured in Four Test Liquids

Liquid or material	δ_2(mm) for Probe Number				Average δ_2(mm) for Liquid (mean ± S.E.)	Calculated δ_2 (mm)†		
	5	6	7B	8B		TE_{10}	TE_{30}	TE_{50}
Gylcerol	10.5	10.4	15.0	15.8	12.9 ± 1.4	13.4 ±1.2	7.1(?)	?
water:glycerol (70:30 v/v) solution	8.5	8.8 7.7 6.2	7.8 8.2	5.8 8.3	7.7 ± 0.4	7.7 ±0.6	7.3	6.5
0.9% (w/w) saline	8.0	8.8	8.7	8.6 7.5	8.3 ± 0.2	8.2	7.9	7.2
water (20°C)	11.7	16.5 14.7	16.0	12.7	14.3 ± 0.9	16.0	15.4	14.1
Probe Average (mean ± S.E.)	9.7 ±0.9	10.4 ±1.4	11.1 ±1.8	9.8 ±1.5				

† From Appendix II

The uncertainty in any single measured δ_2 value is approximately ± 10%.

small but real differences between some of the liquids and probes, as seen in the table. As probes 7B and 8B were replacement probes received at different times after the original set of probes, their fabrication was slightly different. Both had dimensios of 1.20 x 2.47 ($\pm$ 0.03) mm for the substrate cross-section compared to the dimensions 1.20 x 2.35 ($\pm$ 0.03) mm for all of the original set. In addition, probe 7B may have been encased in a somewhat different substrate from the others since it had a distinctively greener colour than the others.

The test solution of most interest is the water-glycerol solution. The average response ratio is 3.00 $\pm$ 0.18 (SE). Taking into account the worst-case bias of $\pm$ 0.6 for any one measurement, the best estimate of the error in the ratio is $+$ 0.6. The response of probe 8B, used for measurements in tissue, can best be estimated by multiplying the best value for B_M/B_A, 3.0 $+$ 0.6, by the ratio of the average response of probe 8B, 2.15, to the average response of the whole group, 2.58, i.e., the best estimate of B_M/B_A for probe 8B for the glycerol-water solution is (3.0 $+$ 0.6) $\times$ (2.15/2.58) = 2.5 $\pm$ 0.5. The result for probe 7B calculated in the same way, is 3.0 $\pm$ 0.6.

The dependence of the probe response ratio on dielectric constant can be seen in Table V. The probes have a slightly lower response in the high-dielectric-constant liquids than in the lower two ones. This is contrary to the published curves of Smith (4), which were calculated for a small cylindrical dipole surrounded by a cylinder of insulator. In comparison, we have a small planar gold-foil dipole surrounded by a relatively thin planar insulator. Our thin-insulator results are more in agreement with his results for "sufficiently thick" insulation, which show that for all $\epsilon' > 6$ the response is independent of ϵ', within 10%. We measured a 20 to 35% ($\pm$ 15%) larger response in liquids of lower ϵ'. In view of the moderate increase involved and the difference in probe geometry, the disagreement between our results and Smith's calculation is not considered important. The most important conclusion is that the response ratio is so nearly independent of ϵ' that the probes can be used in all types of wet (and some dry) tissue without knowing ϵ' at all.

Bassen et al. (2) recently found a probe response ratio (B_M/B_A) of 3.5 for simulated brain material and 5.4 for simulated muscle material in a similar probe used at 2.45 GHz. They also reported a lower response ratio for materials with a lower ϵ' value. As the probe construction was not identical and the dielectric properties have not yet been published, no exact comparison can be made.

Another useful conclusion, deduced from the curves in solution, is that there is no alteration in probe response as the insulated dipole approaches as close as 1.7 mm to the air-solution interface, as predicted by Smith (5).

An attempt was made to determine the dominant higher-order mode in each liquid by comparing the measured value of δ_2 with the values calculated for several TE_{10} modes, as shown in Table VI. The question marks in the row for pure glycerol indicate that it is doubtful if those modes can propagate at all. Allowing for an error of $\pm$ 10% in any single measurement of δ_2, it can be seen that all the single measurements are

$\leq \delta_2$ (TE$_{10}$ mode), as expected.

The standard error in δ_2 for water is 0.9 mm. From Table VII in Appendix II, this corresponds to a temperature change of 2.2°C. Each sample of liquid was used at room temperature, 20.5 ± 1.5 °C, but sample temperature was not measured in each case. It is clear that for water, temperature variation could account for much of the scatter. A similar result likely applies to 0.9% saline and the water-glycerol solution.

The data for glycerol may indicate a TE$_{10}$mode for probes 7B and 8B and a mixture of TE$_{10}$ and TE$_{30}$ modes for probes 5 and 6. The mode of propagation may be sensitive to conditions at the interface. For example, if the thin spacer were slightly curved, although this was never observed, it might excite a different mode.

Because the measured standard errors are comparable to the differe.ce in δ_2 between successive TE$_{mo}$ modes, the propagating mode cannot be determined for certain. It is most likely to be the TE$_{10}$ mode since that mode should be most easily excited by the TE$_{10}$ mode in air on the other side of the thin spacer.

5. USE OF THE PROBES IN DETERMINING ELECTRIC FIELD AND SPECIFIC ABSORPTION RATE IN TISSUE

5.1 RECOMMENDATIONS FOR THE USE OF THE PROBES

Since the probes break easily and cannot be repaired one should take care in all aspects of handling and use. As the miniature cable connectors are awkward to use, care should be taken when connecting the probes. Caution should also be exercised when inserting the probes into tissue and in rotating them, once inserted. They should not be used in an animal that could possibly move and break them. As a precaution against damage, it is a good idea to watch the probe tip during all handling processes.

Electrical burnout problems must also be avoided by using the probes only with a battery-operated digital voltmeter with an input impedance of less than 20 M ohms. As a precaution against charge accumulation and subsequent discharge, the probe tip should never be exposed to microwave radiation when it is not connected through the cable to the meter.

5.2 DETERMINATION OF INTERNAL ELECTRIC FIELD STRENGTH

The relationship between total voltage and total electric field, given in Eq. 3 above, can re-written as

$$E_T^2 = \frac{V_T}{B_M} = \left(\frac{V_T}{B_A} \cdot \frac{B_A}{B_M} \right) \tag{13}$$

Using Eq. 6 to eliminate B_A, we have

$$E_T^2 = \frac{(3770)}{(B_M/B_A)} \left(\frac{V_T}{C_A} \right) \qquad (14)$$

which only contains the measured calibration constants C_A and (B_M/B_A). If C_A were constant, this would be the simplest way to calculate E_T^2. However, since C_A depends slightly on V_T, we can obtain the most useful formula by using Eq. 5 to eliminate the ratio (V_T/C_A). The result is

$$E_T^2 = \frac{(3770)}{(B_M/B_A)} P_d(V_T) \qquad (15)$$

where $P_d(V_T)$ is the power density determined from reading the air calibration curve for the probe in question at the value of V_T measured in tissue.

Probe 8B was used in all tissue measurements. From section 4.4, B_M/B_A is 2.5 ± 0.5 for this probe, giving $E_T^2 = 1508 P_d(V_T)$. Now if $V_T = 10.0$ mV, for example, then from Fig. 5, $P_d = 10.0$ mW/cm^2 and $E_T = 123$ V/m. The error in E_T^2 is $\pm 20\%$ from the factor of 2.5 ± 0.5 and $\pm 10\%$ from the $P_d(V_T)$ calibration errors (from section 2.3) for a total error of $\pm 30\%$. This assumes perfect contact between probe and tissue, or the physiological saline surrounding the tissue.

5.3 DETERMINATION OF SPECIFIC ABSORPTION RATE IN TISSUE

The specific absorption rate (SAR, W/kg) is given in section 1.1, by Eq. 1, as

$$SAR = (\sigma/\rho) E_T^2$$

where σ is the tissue electrical conductivity, shown in Appendix II to be 1.9 ± 0.2 mho/m and ρ is the tissue density, taken to be 1 g/ml = 10^3 kg/m^3, $\pm 5\%$. Combining equations 1 and 15, we obtain

$$SAR = \left(\frac{\sigma}{\rho} \right) \cdot \left(\frac{3770}{B_M/B_A} \right) P_d(V_T) \qquad (16a)$$

$$= \left(\frac{7.15}{B_M/B_A} \right) \cdot P_d(V_T) \qquad (16b)$$

The total uncertainty in SAR, including $\pm 30\%$ from E_T^2, $\pm 10\%$ from σ and $\pm 5\%$ from ρ, is about $\pm 40\%$.

Continuing the previous example for probe 8B with $B_M/B_A = 2.5$ and $V_T = 10.0$ mV, the SAR is 29 ± 11 mW/g, including the total error of $\pm 40\%$.

5.4 MEASUREMENTS OF INTERNAL ELECTRIC FIELD IN MICE

Cairnie et al. (6) have reported a wide range of dosimetry measurements pertaining to the exposure of mice to 2450-MHz radiation under far-field conditions in the NRC Anechoic Chamber. Part of that study involved internal electric field measurements in the testis and abdomen of 13 mice in 5 different orientations.

One major problem became apparent for the use of the probes in tissue - the measurements were quite inconsistent between mice exposed under the same conditions. The standard deviations of the measurements were greater than half the mean in 10/14 cases. This is more than the usual biological variability.

Two explanations for the large scatter in the results are possible. One source of scatter is the inconsistent contact between probe and tissue. As the planar probe tip is rotated in one testis it moves the tissue, changing the shape of the testis and its degree of contact with the probe. Each measurement was likely done with a different area of probe surface in direct contact with tissue, as opposed to small air pockets. The use of physiological saline on the preparation to ensure that no air contacted the probe tip had limited success, partly because the mouse could not usually be oriented to ensure that the saline did not flow away.

The second source of variation might result from the very strong dependence of readings on depth of penetration into the tissue. In one brief test, where the reading for only one probe angle was made, the reading of $V_1 = 7.8$ mV with the dipole about 1 mm into testis reduced to a constant 1.2 mV at 3 or 4 mm into the tissue. This 2- or 3-mm decay distance is much less than the value of $\delta_2 = 9.6$ mm calculated for the decay of E^2 for a plane wave penetrating a flat surface of material with dielectric properties equal to testis. The effect may have been due to the curvature of the surface or to changes in probe contact. In any case, distance into the testis, which may be crucial, could not be precisely controlled in those experiments.

6. CONCLUSIONS AND RECOMMENDATIONS

6.1 S-BAND WAVEGUIDE CALIBRATION TECHNIQUE

6.1.1. Conclusions for Probe Calibration in Air

(i) The results of the measurements in waveguide, where the ratio $E/H \neq 377$ ohms, must be converted to the power density equivalent to free space using the known correction factor, λ_g/λ. This correction is accurate and easy to apply.

(ii) The results of air calibration measurements performed in three different ways by two groups - ourselves and Narda Microwave - agreed within the experimental errors.

(iii) Our waveguide technique for air calibration is easier than, and more accurate than, our anechoic chamber technique (± 10% compared

to ± 18%, respectively). The difference is not important, however, since most animal experiments involve the use of the same power density meters which gave rise to the ± 18% error in anechoic chamber calibrations in the first place.

6.1.2 Conclusions for Probe Calibration in Tissue-Equivalent Liquids

(i) The probe response ratio, B_M/B_A, is determined by a direct method involving only the continuity of tangential electric field at an interface. The zero of position on each side of the interface is set by measuring a standing wave pattern with air on both sides of the interface.

(ii) Any spacer thickness less than 1.4 mm is likely satisfactory. A 0.25-mm spacer was used in all tests.

(iii) Care is required in setting and measuring position, and in filling the test cell to the correct height of liquid.

(iv) The method is very well suited to studying response as a function of dielectric constant.

(v) The measurements in liquids always showed an exponential decay, i.e., a straight line on semilog paper. The measurements in air were curves on semilog paper, giving rise to appreciable extrapolation error.

(vi) The measured δ_2 values are reasonable, but due to the effects of temperature and the close spacing of the δ_2 values for the higher order modes, the measured δ_2 cannot be used to precisely determine the actual higher order mode propagating. The TE_{10} mode is likely the only propagating mode.

6.1.3 Recommendations for Future Work in Tissue-Equivalent Liquids

(i) Additional accurate data on the dielectric properties of pure liquids and solutions is required at 2450 MHz.

(ii) Tests in liquids at higher temperatures could be used to check the effect of tissue temperatures near 35 to 40 °C on probe response.

(iii) For further work to identify which higher-order modes are propagating: liquid temperatures must be controlled and measured; a thicker spacer should be tried to ensure no bending of the spacer interface; and the VSWR on the air side of the interface should always be measured as a check on the consistency of the propagating mode patterns.

6.1.4 Comparison with the Technique of Bassen et al.

Bassen et al. (2) measured fields through the center of a sphere of tissue-equivalent phantom material exposed in an anechoic chamber. The following comparisons are made:

(i) Both techniques require the construction of a small amount of specilized equipment.

(ii) They had to use a low-pass 0.5-Hz filter to reduce noise resulting from flexure of the probe as it was moved through the sphere. We had no such problem. A new prototype rigid probe design has significantly reduced flexure noise.

(iii) For materials equivalent to wet tissue, our probe response ratio of 3.0 ± 0.6 agrees with their value of 3.6 for brain-equivalent material, but disagrees with their value of 5.4 for muscle-equivalent material.

(iv) The waveguide and sphere techniques are complementary, each having its own advantages and disadvantages. The advantages of the waveguide technique are: (1) The test liquids are easier to work with than the semi-solid materials used in the sphere method; (2) The calculation of the field pattern on both sides of the air-liquid interface is much simpler than the calculation for inside the sphere; (3) The comparison of the measured and calculated δ_2 values provides a check on the accuracy of the measured (or assumed) dielectric properties; (4) The errors in the method can easily be assessed.

The advantages of the sphere technique are: (1) Spatial averaging is done over the non-uniform field distribution; (2) The extrapolation of measured curves to locations inaccessible to the probe dipole is avoided; (3) The peak E field is located by passing through it.

6.2 PERFORMANCE EVALUATION FOR THE BRH-NARDA MINIATURE ELECTRIC FIELD PROBE

6.2.1 Performance in Air

(i)   Probe output voltage has been found to be proportional to E_T^{2n}, from 0.5 to 15 mV, with a slightly decreasing response above 15 mV. The value of n is 0.95 ± 0.02, very close to unity.

(ii) Probe sensitivity ranges from 0.89 to 1.31 $mV/mWcm^{-2}$ for the five probes tested. The difference is large enough that a separate calibration curve is needed for each probe.

(iii) The small probe size makes it useful for measuring fields in any location which cannot be reached by conventional power density meters because of their large, 5-cm-diameter, sensors.

6.2.2 Response in Tissue-Equivalent Liquids

(i)   The increased probe response in tissue-equivalent liquids is expressed as the "probe response ratio", B_M/B_A. This was found to be approximately independent of the liquid's dielectric constant, within ± 15%, including values of dielectric constant as low as 6.3 (for glycerol). This result differs from Bassen's (2) and also does not agree with Smith's calculation (5) for a cylindrical dipole inside an electrically small cylinder of insulator. As our dipole is a thin foil embedded in a thin planar insulator, the geometry is sufficiently different that another result might be expected. Because response is independent of dielectric constant, the probes can be used in any wet or dry tissue where they can be inserted without breaking.

(ii)   The overall average value of B_M/B_A measured for four probes in four test liquids is 2.57 ± 0.11.   Including possible bias in the zero of position measurements, the error is more likely about ± 0.4, which we consider acceptable.

(iii) The best model for wet tissue is the water-glycerol solution (70:30 v/v) which has $\epsilon' = 58.5$, $\epsilon'' = 19.5$ and $B_M/B_A = 3.00 \pm 0.18$ (mean ± SE for 7 measurements with 4 probes).

(iv)   The response ratio averaged over all liquids was found to be almost independent of probe.   Only probe 8B ($B_M/B_A = 2.15 \pm 0.14$ (N = 6)) differed significantly (t = 2.698, 20 d.f., p < 0.05) in its response from the average of the other three probes ($B_M/B_A = 2.73 \pm 0.12$ (N = 16)). Other workers using their own set of similar probes need not calibrate them in tissue-equivalent liquids - it would not be worth the effort.

(v)   There is no problem using the probes near an interface between any two different materials.   The response did not change when the probe was brought as close as 1.7 mm to an air-liquid interface, in agreement with Smith (5).

6.2.3   Results in Tissue

(i)   The experience of Cairnie et al. (6) making measurements in mouse abdomen and testis indicates it is difficult to obtain good reproducibility of measurements.   This may result from irregular tissue contact or a strong dependence of results on probe depth in tissue.

(ii)   To improve the consistency of tissue contact, the mouse should always be used prone so that applied saline will not run off.   This necessitates the creation of an electric field in the anechoic chamber of either vertical or horizontal polarization, depending on the mouse orientation being investigated.

(iii) An attempt should be made to control more precisely the probe depth and position.

6.3   RECOMMENDATIONS FOR IMPROVEMENTS IN PROBE DESIGN

(i)   A more rugged mechanical construction for the probes is essential to prevent breakage.   This has been done for the newer versions of the probe.

(ii)   If other users have also had problems with electrical burnout of probes, this problem must be investigated and solved.   It does not seem likely that the problem lies with our electrometer, since all our tests indicate it is functioning properly.

(iii) The Microtech EP-7S-1 six-pin miniature connector has been found very awkward to use.   There is too great a danger of dropping the probe or hitting the tip against something while struggling to connect or disconnect the cable, particularly for inexperienced operators.   A new 2-pin connector should be selected.

(iv)   Rotating the flat probe tip in tissue increases the chance of tip breakage. It also may change the degree of contact between probe and tissue which would greatly affect the readings. If the last 5 cm of the probe were made into a rigid, pointed cylinder, this would make insertion easier and the contact more consistent. This has been done for one of the newer versions of the probe.

(v)   The tip diameter, just less than 3 mm, is too large for use in many small-animal organs, such as the testis of a mouse.

REFERENCES

1. H. Bassen, P. Herchenroeder, A. Cheung and S. Neuder. "Evaluation of an implantable electric-field probe within finite simulated tissues." Radio Science 12, No. 6(S), 15-25 (1977).

2. H. Bassen, K. Franke, T.W. Aphey and E. Aslan. "An improved implantable electric field probe." BRH draft internal report. (US) Bureau of Radiological Health (1980).

3. H.M. Assenheim and G.W. Hartsgrove. "The design and evaluation of an anechoic chamber for the irradiation of small and large animals." National Research Council of Canada Report No. 17448, (1979).

4. G.S. Smith. "A comparison of electrically short bare and insulated probes for measuring the local radiofrequency electric field in biological systems." IEEE Transactions on Biomed. Engineering, BME-22, 477-483 (1975).

5. G.S. Smith. "The electric-field probe near a material interface with application to the probing of fields in biological bodies." IEEE Transactions on Microwave Theory and Technique, MTT-27, 270-278 (1979).

6. A.B. Cairnie, D.A. Hill and H.M. Assenheim. "Dosimetry for a study of effects of 2.45-GHz microwaves on mouse testis." Bioelectromagnetics, accepted for publication in Vol. 1, No. 3, (1980).

7. T. Moreno. Microwave Transmission Design Data, 1st edn., McGraw-Hill (1948). Also reprinted by Dover in 1958.

8. C.K. Chou and A.W. Guy. "Effects of electromagnetic fields on isolated nerve and muscle preparations." IEEE Transactions on Microwave Theory and Techniques, MTT-26, 141-147 (1978).

9. J.P. Hasted. Aqueous Dielectrics. Chapman and Hall (1973).

10. C.C. Johnson and A.W. Guy. "Non-ionizing electromagnetic wave effects in biological materials and systems." Proc. IEEE 60 No. 6, 692-718 (1972).

11. M. Brady, G. Gajda, A. Thansandote and S.S. Stuchly. Private communication, (1980). Preliminary measurements of the dielectric properties of glycerol and water-glycerol solutions using a new probe technique. Their data is used in Tables VI and VII.

APPENDIX I

CALCULATION OF POWER DENSITY IN AIR-FILLED WAVEGUIDE

For a TE_{10} mode travelling along a waveguide with a (reflectionless) matched load, the electric (E) and magnetic (H) field patterns have been described by Moreno (7, p 113). The (x, y, z) co-ordinate system has the origin at one inside corner of the waveguide. The x-axis runs from "0" to "a" across the broad face of the waveguide. The y-axis runs from "0" to "b" across the narrow face of the waveguide, and the z-axis runs the length of the waveguide.

The E- and H-field patterns are given by

$$E_y = E_o \sin(\pi x/a)\sin(\omega t - \beta z)$$
$$H_x = H_o \sin(\pi x/a)\sin(\omega t - \beta z)$$
$$E_x = E_z = H_y = 0 \qquad (17)$$
$$H_z \neq 0 \text{ (but is not needed).}$$

Here, ω is the microwave angular frequency (rad/sec), β is the propagation constant and E_o and H_o are constants to be determined.

The net power flow along the waveguide may be calculated from the z component of the Poynting vector;

$$\vec{S} = \vec{E} \times \vec{H} \qquad (18)$$

$S_z(x,y,t)$ is the instantaneous energy flow per unit area (W/m^2).

$$S_z(x,y,t) = E_x H_y - E_y H_x \qquad (19)$$

$= -E_y H_x$, since E_x is zero everywhere. The minus sign, which just indicates the direction of energy flow, will be dropped, leaving

$$S_z(x,y,t) = E_o H_o \sin^2(\pi x/a)\sin^2(\omega t - \beta z). \qquad (20)$$

Defining the power density, $P_d(x,y)$ as the time average of $S_z(x,y,t)$ over one cycle of oscillation, and defining $P_d(c)$ as the power density at the center of the waveguide, the above equation reduces to

$$P_d(x,y) = P_d(c)\sin^2(\pi x/a), \text{ with} \qquad (21)$$

$$P_d(c) = P_d(x = a/2, y = b/2) = E_o H_o /2 \qquad (22)$$

$$= E_c H_c \qquad (23)$$

where E_c and H_c are the rms E- and H-field strengths at the center of the waveguide.

Defining P_o as the net power flow along the waveguide, it is calculated as the integral of the power density over the cross-sectional area of the waveguide i.e.,

$$P_o = \int_o^b \int_o^a P_d'(x,y) \, dx \, dy \tag{24}$$

$$= a \, b \, P_d' \, (c)/2. \tag{25}$$

Rearranging equation 25 gives

$$P_d' \, (c) = \frac{2P_o}{ab} = \frac{2P_o}{A}, \text{ where} \tag{26}$$

$A = ab$ is the cross-sectional area of the waveguide.

For the TE_{10} waveguide mode the characteristic wave impedance is not the same as $Z_o = 377$ ohms, which applies to waves in free space. It is given by Moreno (7, p 34) as

$$E_y/H_x = Z = Z_o \, (\lambda_g/\lambda) \tag{27}$$

for all x and y. λ, the free-space wavelength, and λ_g, the guide wavelength, are related to each other and the cut-off wavelength, λ_c, by the well known (Moreno 7, p 123) relationship

$$\frac{1}{\lambda^2} = \frac{1}{\lambda_g^2} + \frac{1}{\lambda_c^2} \tag{28}$$

where $\lambda_c = 2a$.

Applying the definition of Z to the power density formula gives

$$P_d' \, (c) = E_c \, H_c = E_c^2/Z = ZH_c^2. \tag{29}$$

Since the probes actually measure E^2, not P_d', and since $Z \neq Z_o$, the calibration in waveguide must be corrected to relate it to the power density at the center of the waveguide equivalent to the free-space situation, $P_d \, (c)$, defined using Z_o.

From equations 27 and 39 we have

$$P_d \, (c) = \frac{E_c^2}{Z_o} = P_d' \, (c) \left(\frac{\lambda_g}{\lambda} \right) \tag{30}$$

The formulas will now be evaluated for the case of a forward power of $P_o = 1$ watt, a frequency of 2450 MHz, and standard S-band waveguide (WR-284).

$$a = 7.214 \text{ cm}$$

$$b = 3.40 \text{ cm}$$

$$\lambda_c = 2a = 14.43 \text{ cm}$$

$$A = ab = 24.51 \text{ cm}^2$$

$$P_o = 1 \text{ watt}$$

$$\lambda = 12.24 \text{ cm}$$

$$\lambda_g = 23.09 \text{ cm}$$

$$\lambda_g / \lambda = 1.89$$

$$Z = Z_o \left(\frac{\lambda_g}{\lambda}\right) = (377 \text{ ohms})(1.89) = 713 \text{ ohms}$$

$$E_c = 762 \text{ V/m (rms)}$$

$$H_c = 1.070 \text{ A/m (rms)}$$

$$P'_d \text{ (c)} = 816 \text{ W/m}^2 = 81.6 \text{ mW/cm}^2$$

$$P_d \text{ (c)} = 154 \text{ mW/cm}^2$$

Changing the frequency by 10 MHz to 2440 MHz makes $\lambda_g/\lambda = 1.91$, only 1% different from 1.89, so the effect of small changes in frequency are ignored in this work.

APPENDIX II

DIELECTRIC PROPERTIES AND CALCULATED DEPTH OF PENETRATION

FOR 2450-MHz RADIATION IN VARIOUS MEDIA

The dielectric properties and calculated depth of penetration for several different modes of propagation in various materials of interest are listed in Table VII. The goal of the calculation is to attempt to identify the actual mode propagating in the liquid by comparing the measured δ_2 value to the calculated ones for the various modes.

The standard complex number notation for electromagnetic waves propagating in any homogeneous isotropic medium is used in this Appendix. The complex dielectric constant, or relative permittivity, is therefore defined as $\varepsilon = \varepsilon' - j\varepsilon''$. The electrical conductivity, σ, is given by $\sigma = \omega\varepsilon''\varepsilon_0$, where ε_0 = 8.85 picofarad/m, $\omega = 2\pi f$, and f = 2.45 GHz. With σ expressed in mho/m, this reduces to $\varepsilon'' = 7.34\ \sigma$.

The tabulated dielectric properties are taken from the references given. Since ε'' and σ are both in common usage, both are given. For physiological saline (9 g/l NaCl), the data of Chou and Guy (8) for mammalian Ringer solution are used, as the two solutions are electrically very similar. Testis was assumed to have properties equal to the average of skeletal muscle and liver, two other wet tissues that have been measured at frequencies near 2.45 GHz. In particular, the muscle and liver data quoted by Hasted (9, p 229) for 1.00 and 3.00 GHz were used in a linear interpolation calculation. The dielectric properties of water were calculated using linear interpolation in temperature and frequency from the data of three different papers quoted by Hasted (9, pp. 43-45). The data included frequencies of 1.744, 2.61 and 3.00 GHz and temperatures of 20, 25, 30 and 40 °C.

The propagation of different modes in waveguide, when described using the complex number notation, has E- and H-fields which vary along the waveguide as $\exp(-\gamma z)$. γ, the propagation constant, is a complex number written as

$$\gamma = \alpha + j\beta \tag{1}$$

where α is the "attenuation constant" and β is the "phase constant". α and β are real numbers with dimensions of inverse length. For a mode propagating in a waveguide completely filled with a homogeneous, isotropic material of complex dielectric constant ε, γ is given by

$$\gamma = (2\pi/\lambda)((\lambda/\lambda_c)^2 - \varepsilon)^{\frac{1}{2}} \tag{2}$$

where λ_c is the cut-off wavelength for the mode in question in an air-filled waveguide. Since λ = 12.24 cm this reduced to

$$\gamma = 0.513\ cm^{-1}((12.24/\lambda_c)^2 - \varepsilon' + j\varepsilon'')^{\frac{1}{2}} \tag{3}$$

TABLE VII

Calculation of λ_2 for 2450-MHz Radiation Propagating in

Different Modes in Different Materials

Liquid or Material	T (°C)	Dielectric Properties			Reference	λ_2 (mm) Propagation mode and $(\lambda/\lambda_c)^2$			
		ε'	ε''	σ (mho/m)		TEM 0	TE10 0.72	TE30 6.48	TE50 18.0
wet tissue	37	47	16.2	2.21	Johnson & Guy (10)	8.4 8.5†	8.3		
gylcerol	23	6.3 ±0.3	3.6 ±0.4	0.49 ±0.05	Brady et al. (11)	14.1	13.4 ±1.2	7.1(?)	(?)
water:glycerol (70:30, v/v)	23	58.5 ±1.0	19.5 ±1.5	2.66 ±0.20	"	7.7	7.7 ±0.6	7.3	6.5
testis	37	45.6 ±1.0	13.9 ±1.5	1.9 ±0.2	See text	9.6	9.5		
0.9% saline	23	74.3	20.5	2.79	Chou & Guy (8) (Mammalian Ringer)	8.2 8.2†	8.2	7.9	7.2
water	20 25 40	78.50 77.2 72.7	10.76 9.45 6.2	1.47 1.29 0.84	Tables in Hasted (9) pp. 43-45	16.1 18.2 26.8	16.0 18.1 26.7	15.4 17.4 25.6	14.1 15.9 23.3

† derived from the author's determination of λ_1 by taking $\lambda_2 = \lambda_1/2$.

The same equation applies to the propagation of a TEM mode in an unbounded medium when λ_c is set equal to infinity, which applies to the actual situation in tissue.

Many higher-order modes can propagate in liquid-filled waveguide. For example, for $\varepsilon = 49 - j0$, $\sqrt{\varepsilon^T} = 7$ and TE_{mo} modes as high as the TE_{80} mode may propagate. In our case, since the TE_{10} mode is the only mode present on the air side of the interface, we expect most of the energy to go into the TE_{mo} modes in solution, but not necessarily the TE_{10} mode. The cut-off wavelength for the TE_{mo} mode in air-filled waveguide, denoted λ_{cmo}, can easily be shown (Moreno (7), p 120) to be given by

$$\lambda_{cmo} = \frac{2a}{m} = \frac{14.43 \text{ cm}}{m} .\tag{34}$$

Using the values $\lambda_{c10} = 14.43$ cm, $\lambda_{c30} = 4.81$ cm and $\lambda_{c50} = 2.89$ cm, δ_2 for each of the corresponding modes in each test liquid was calculated.

δ_2 for the TEM mode in an unbounded medium is also given in the table to show that it never differs appreciably from the value for the TE_{10} mode.

The significant effect of temperature on δ_2 can be seen in the table for water, where the rate of change of δ_2 is 0.4 mm/deg C.

DOCUMENT CONTROL DATA - R & D

(Security classification of title, body of abstract and indexing annotation must be entered when the overall document is classified)

1. ORIGINATING ACTIVITY	2a. DOCUMENT SECURITY CLASSIFICATION
Defence Research Establishment Ottawa Ottawa, Ontario K1A 0Z4	Unclassified 2b. GROUP N/A

3. DOCUMENT TITLE

TECHNIQUE FOR CALIBRATING MINIATURE ELECTRIC-FIELD PROBES FOR USE IN MICROWAVE BIOEFFECTS STUDIES AT 2450 MHz: EVALUATION AND CALIBRATION OF BRH - NARDA PROBES (U)

4. DESCRIPTIVE NOTES (Type of report and inclusive dates)

Technical Note

5. AUTHOR(S) (Last name, first name, middle initial)

Hill, Douglas A. and Hartsgrove, George W.

6. DOCUMENT DATE	7a. TOTAL NO OF PAGES	7b. NO OF REFS
Dec 80	33	11

8a. PROJECT OR GRANT NO	9a. ORIGINATOR'S DOCUMENT NUMBER(S)
16C	DREO-TN- 80-31

8b. CONTRACT NO	9b. OTHER DOCUMENT NO (S) (Any other numbers that may be assigned this document)

10. DISTRIBUTION STATEMENT

Unlimited distribution

11. SUPPLEMENTARY NOTES	12. SPONSORING ACTIVITY
	CRAD

13. ABSTRACT

A set of miniature probes for determining electric fields in tissue was evaluated and calibrated for use in microwave bioeffects studies at 2450 MHz. The calibrations in air and tissue-equivalent liquids were carried out using a new S-band waveguide technique. The air calibration using waveguide has an accuracy of $\pm$ 10% compared to $\pm$ 18% for our anechoic-chamber calibration. The average probe sensitivity in air is 1.0 mV/mWcm^{-2} for the five probes calibrated and varies slightly with power density and probe. To estimate probe sensitivity in tissue, a section of waveguide is filled with a tissue-equivalent liquid and is separated from the air-filled waveguide by a very thin (0.25 mm) planar spacer. The probe response is measured as a function of position on either side of the spacer and extrapolated to the interface. The ratio of probe sensitivity in air to that in test liquid is then determined using the continuity of tangential E field across the spacer. Liquids with dielectric properties simulating both wet and dry tissues were used. For the water-glycerol solution modelling wet tissue the probes are 3.0 $\pm$ 0.6 times more sensitive to E^2 than for air. When used in tissue the total calibration error is estimated to be $\pm$ 30% for E^2 and $\pm$ 40% for the specific absorption rate at the site. One of the problems with this probe design, the mechanical weakness near the tip, has been eliminated in newer designs. The other problem, that the size of the probe tip ($\sim$3 mm) is too large for optimal use in small-animal organs, is more difficult to solve. (U)

DSIS

KEY WORDS

(1) microwave

(2) bioeffect

(3) electric field

(4) waveguide

INSTRUCTIONS

1. ORIGINATING ACTIVITY Enter the name and address of the organization issuing the document.

2a. DOCUMENT SECURITY CLASSIFICATION Enter the overall security classification of the document including special warning terms whenever applicable.

2b. GROUP Enter security reclassification group number The three groups are defined in Appendix 'M of the DRB Security Regulations.

3. DOCUMENT TITLE Enter the complete document title in all capital letters Titles in all cases should be unclassified If a sufficiently descriptive title cannot be selected without classification, show title classification with the usual one capital letter abbreviation in parentheses immediately following the title.

4. DESCRIPTIVE NOTES Enter the category of document, e.g. technical report, technical note or technical letter If appropriate, enter the type of document, e.g. interim, progress, summary, annual or final Give the inclusive dates when a specific reporting period is covered.

5. AUTHOR(S) Enter the name(s) of author(s) as shown on or in the document Enter last name, first name, middle initial If military, show rank The name of the principal author is an absolute minimum requirement.

6. DOCUMENT DATE Enter the date (month, year) of Establishment approval for publication of the document.

7a. TOTAL NUMBER OF PAGES The total page count should follow normal pagination procedures, i.e enter the number of pages containing information.

7b. NUMBER OF REFERENCES Enter the total number of references cited in the document.

8a. PROJECT OR GRANT NUMBER If appropriate, enter the applicable research and development project or grant number under which the document was written.

8b. CONTRACT NUMBER If appropriate, enter the applicable number under which the document was written.

9a. ORIGINATOR'S DOCUMENT NUMBER(S) Enter the official document number by which the document will be identified and controlled by the originating activity This number must be unique to this document.

9b. OTHER DOCUMENT NUMBER(S) If the document has been assigned any other document numbers (either by the originator or by the sponsor), also enter this number(s).

10. DISTRIBUTION STATEMENT Enter any limitations on further dissemination of the document, other than those imposed by security classification, using standard statements such as

  (1) "Qualified requesters may obtain copies of this document from their defence documentation center."

  (2) "Announcement and dissemination of this document is not authorized without prior approval from originating activity."

11. SUPPLEMENTARY NOTES Use for additional explanatory notes.

12. SPONSORING ACTIVITY Enter the name of the departmental project office or laboratory sponsoring the research and development. Include address.

13. ABSTRACT Enter an abstract giving a brief and factual summary of the document, even though it may also appear elsewhere in the body of the document itself It is highly desirable that the abstract of classified documents be unclassified Each paragraph of the abstract shall end with an indication of the security classification of the information in the paragraph (unless the document itself is unclassified) represented as (TS), (S), (C), (R), or (U).

  The length of the abstract should be limited to 20 single spaced standard typewritten lines, 7½ inches long.

14. KEY WORDS Key words are technically meaningful terms or short phrases that characterize a document and could be helpful in cataloging the document Key words should be selected so that no security classification is required Identifiers, such as equipment model designation, trade name, military project code name, geographic location, may be used as key words but will be followed by an indication of technical context.

DA
FILM